

## Retraction

# Retracted: 2D-DOA Estimation for EMVS Array with Nonuniform Noise

### International Journal of Antennas and Propagation

Received 19 December 2023; Accepted 19 December 2023; Published 20 December 2023

Copyright © 2023 International Journal of Antennas and Propagation. This is an open access article distributed under the Creative Commons Attribution License, which permits unrestricted use, distribution, and reproduction in any medium, provided the original work is properly cited.

This article has been retracted by Hindawi following an investigation undertaken by the publisher [1]. This investigation has uncovered evidence of one or more of the following indicators of systematic manipulation of the publication process:

- (1) Discrepancies in scope
- (2) Discrepancies in the description of the research reported
- (3) Discrepancies between the availability of data and the research described
- (4) Inappropriate citations
- (5) Incoherent, meaningless and/or irrelevant content included in the article
- (6) Manipulated or compromised peer review

The presence of these indicators undermines our confidence in the integrity of the article's content and we cannot, therefore, vouch for its reliability. Please note that this notice is intended solely to alert readers that the content of this article is unreliable. We have not investigated whether authors were aware of or involved in the systematic manipulation of the publication process.

Wiley and Hindawi regrets that the usual quality checks did not identify these issues before publication and have since put additional measures in place to safeguard research integrity.

We wish to credit our own Research Integrity and Research Publishing teams and anonymous and named external researchers and research integrity experts for contributing to this investigation.

The corresponding author, as the representative of all authors, has been given the opportunity to register their agreement or disagreement to this retraction. We have kept a record of any response received.

### References

- [1] C.-X. Cai, G.-J. Huang, F.-Q. Wen, X.-H. Wang, and L. Wang, "2D-DOA Estimation for EMVS Array with Nonuniform Noise," *International Journal of Antennas and Propagation*, vol. 2021, Article ID 9053864, 9 pages, 2021.

## Research Article

# 2D-DOA Estimation for EMVS Array with Nonuniform Noise

Chang-Xin Cai,<sup>1</sup> Guan-Jun Huang ,<sup>1</sup> Fang-Qing Wen ,<sup>2</sup> Xin-Hai Wang,<sup>3</sup> and Lin Wang<sup>4</sup>

<sup>1</sup>National Demonstration Center for Experimental Electrical and Electronic Education, Yangtze University, Jingzhou 434200, China

<sup>2</sup>College of Computer and Information Technology, China Three Gorges University, Yichang 443002, China

<sup>3</sup>Nanjing Marine Radar Institute, Nanjing 211153, China

<sup>4</sup>The 723 Institute of CSIC, Yangzhou 225000, China

Correspondence should be addressed to Guan-Jun Huang; 201971326@yangtzeu.edu.cn

Received 21 June 2021; Revised 24 July 2021; Accepted 9 August 2021; Published 19 August 2021

Academic Editor: Jin He

Copyright © 2021 Chang-Xin Cai et al. This is an open access article distributed under the Creative Commons Attribution License, which permits unrestricted use, distribution, and reproduction in any medium, provided the original work is properly cited.

Electromagnetic vector sensor (EMVS) array is one of the most potential arrays for future wireless communications and radars because it is capable of providing two-dimensional (2D) direction-of-arrival (DOA) estimation as well as polarization angles of the source signal. It is well known that existing subspace algorithm cannot directly be applied to a nonuniform noise scenario. In this paper, we consider the 2D-DOA estimation issue for EMVS array in the presence of nonuniform noise and propose an improved subspace-based algorithm. Firstly, it recasts the nonuniform noise issue as a matrix completion problem. The noiseless array covariance matrix is then recovered via solving a convex optimization problem. Thereafter, the shift invariant principle of the EMVS array is adopted to construct a normalized polarization steering vector, after which 2D-DOA is easily estimated as well as polarization angles by incorporating the vector cross-product technique and the pseudoinverse method. The proposed algorithm is effective to EMVS array with arbitrary sensor geometry. Furthermore, the proposed algorithm is free from the nonuniform noise. Several simulations verify the improvement of the proposed method.

## 1. Introduction

Sensor array is one of the most important infrastructures in wireless communication and radar detection [1–4]. Among the various branches in array signal processing, direction-of-arrival (DOA) estimation is the most canonical one and has aroused much attention. The principle of DOA estimation is to estimate the direction of the incoming source via the phase characteristics between sensors, and it is a highly nonlinear problem. Many efforts have been devoted to tackling this issue, for instance, an estimation approach to signal parameters with the rotational invariance technique (ESPRIT) [5, 6], Capon, multiple signal classification (MUSIC) [7–9], propagator method (PM) [10], maximum-likelihood (ML) [11], and tensor method [12–14]. Usually, the spectrum search counterparts, such as MUSIC, are always inefficient. Besides, they hardly avoid the off-grid problem. ESPRIT, however, is much more efficient than the

spectrum search frameworks because it can acquire closed-form solutions to the parameter estimation issue.

A majority of the current studies focus on how to estimate the one-dimensional (1D) DOA from the scalar sensor arrays, e.g., uniform linear array (ULA). In practice, two-dimensional (2D) DOA may be more attractive. To pursue 2D-DOA estimation with the traditional scalar sensors, nonlinear sensor geometries are necessary [15–17], e.g., L-shape array, circular geometry, and rectangular manifold. Unfortunately, scalar sensor arrays often suffer from the sensor position error. Thus, complex array calibration is indispensable. Unlike scalar sensors, a single electromagnetic vector sensor (EMVS) is capable of providing 2D-DOA estimation [18]. Moreover, it is able to offer additional polarization angles of the source, and such characteristic may be very helpful in detecting stealth source [19]. Besides, an EMVS array with  $N$  sensors occupies more degree of freedom (DOF) than a scalar array, and thus, it

provides more accurate estimation result than the latter. Furthermore, it has been proven that parameter estimation using EMVS array is insensitive to sensor positions [20], giving rise to the fact that the EMVS is more flexible than the traditional scalar sensor arrays.

It should be emphasized that the angle estimation issue using EMVS array is often more complex than that using the scalar sensors, since it involves 2D-DOA (azimuth angle and elevation angle) and 2D polarization angle (polarization phase difference and auxiliary polarization angle). In [19], the vector cross product was proposed, and the angles therein were obtained from the Poynting vector of the polarization steering vector. In [20], the ESPRIT-like algorithm was introduced. Therein, the concept of normalized Poynting vector was proposed to estimate the 2D-DOA, which was insensitive to the sensor positions and free from the sensor position error. In [21], the ULA-configured EMVS architecture was presented, and another ESPRIT estimator was derived. Unlike [20], the elevation angle was achieved by using ESPRIT, and the azimuth angle was estimated by using vector cross product. Likewise, in [22–26], the methods of combining the subspace approach and vector cross product were investigated. To avoid the eigendecomposition in the subspace approaches, a PM-like algorithm was presented in [27]. To further exploit the multidimensional structure in EMVS array, tensor algorithms were also been investigated in [28]. Besides, some efforts have been devoted to the active radar system with EMVS arrays [29–31], which brings new insights to target detection.

Nevertheless, it should be noticed that the subspace-based approaches achieve good performance with Gaussian white noise. In practice, the array noise may be nonuniform due to hardware nonideality. The nonuniform noise issue has been extensively stressed in scalar sensor array [32–35], but little attention has been paid to EMVS array. Therefore, we revisit the 2D-DOA estimation in EMVS array with nonuniform noise in this paper. An improved ESPRIT algorithm is presented. It eliminates the nonuniform noise via constructing a reduced covariance matrix, after which both noise covariance and parts of the signal covariance are removed. The recovery of the noiseless covariance matrix is recast as a matrix completion issue and is accomplished via solving a convex optimization problem. Thereafter, the ESPRIT idea is adopted to construct the normalized polarization steering vector. 2D-DOA, as well as polarization parameters, is then achieved by combining the vector cross product and the least squares (LS) technique. Our algorithm is effective in the scenario with arbitrary array geometry. Numerical simulations are designed to verify its effectiveness.

## 2. Preliminaries and the Data Model

**2.1. EMVS Preliminaries.** For a complete EMVS, it consists of six collocated antennas: three electric dipoles, and three magnetic loops. The dipoles and loops, respectively, sense the information of the electric field and magnetic field. Considering that a far-field source signal impinges on a

single EMVS, the polarization responses of the six components can be expressed as

$$b = \left[ \underbrace{b(1) \ b(2) \ b(3)}_{e \in \mathbb{C}^{3 \times 1}} \ \underbrace{b(4) \ b(5) \ b(6)}_{m \in \mathbb{C}^{3 \times 1}} \right]^T, \quad (1)$$

$$= Dp,$$

where  $(\cdot)^T$  denotes transpose.  $D$  and  $p$  are, respectively, given by

$$D = \begin{bmatrix} \cos \phi \cos \theta & -\sin \phi \\ \sin \phi \cos \theta & \cos \phi \\ -\sin \theta & 0 \\ -\sin \phi & -\cos \phi \cos \theta \\ \cos \phi & -\sin \phi \cos \theta \\ 0 & \sin \theta \end{bmatrix} \quad (2)$$

and

$$p = \begin{bmatrix} \sin \gamma e^{j\eta} \\ \cos \gamma \end{bmatrix}, \quad (3)$$

where  $e$  and  $m$  denote the electric steering vector and the magnetic steering vector, respectively;  $\theta$ ,  $\phi$ ,  $\gamma$ , and  $\eta$  denote, respectively, the elevation angle, the azimuth angle, the auxiliary polarization angle, and the polarization phase difference.  $D \in \mathbb{C}^{6 \times 2}$  denotes the direction-only matrix, and  $p \in \mathbb{C}^{2 \times 1}$  denotes the polarization-only vector, respectively. Moreover, the Poynting vector between  $e$  and  $p$  satisfies [20]

$$\frac{e}{|e|} * \frac{p^*}{|p|} = \begin{bmatrix} \sin \theta \cos \phi \\ \sin \theta \sin \phi \\ \cos \theta \end{bmatrix}, \quad (4)$$

where  $(\cdot)^*$  denotes the conjugate,  $|\cdot|$  returns the absolute value, and  $*$  denotes the vector cross product.

**2.2. Data Model.** Let us consider an  $N$ -element EMVS array. Without loss of generality, let the coordinate of the  $n$ -th EMVS be  $r_n = [x_n, y_n, z_n]^T$ . Suppose that  $K$  far-field signals appear in the array. Let  $\theta_k$ ,  $\phi_k$ ,  $\gamma_k$ , and  $\eta_k$  stand for the  $k$ -th ( $k = 1, 2, \dots, K$ ) angle parameters. The array signal can be written as [19]

$$y(t) = \sum_{k=1}^K [a_k \otimes b_k] s_k(t) + n(t), \quad (5)$$

where  $t$  is the time index;  $\otimes$  denotes the Kronecker product,  $a_k = [e^{-j\pi\tau_{1,k}}, e^{-j\pi\tau_{2,k}}, \dots, e^{-j\pi\tau_{N,k}}]^T$ , where  $\tau_{n,k} = r_n^T g_k / \lambda \in \mathbb{C}^{N \times 1}$  denotes the  $k$ -th spatial response (steering) vector with  $g_k = [\cos(\phi_{t,k})\sin(\theta_{t,k}), \sin(\phi_{t,k})\sin(\theta_{t,k}), \cos(\theta_{t,k})]^T$  and  $\lambda$  is the carrier wavelength; and  $b_k = D_k v_k$  denotes the polarization response vector associated with the  $k$ -th target.  $s_k(t)$  accounts for the  $k$ -th signal;  $n(t)$  denotes the array noise. Let  $A = [a_1, a_2, \dots, a_K] \in \mathbb{C}^{N \times K}$  and  $B = [b_1, b_2, \dots, b_K] \in \mathbb{C}^{6 \times K}$ . Equation (6) can also be formulated as

$$\begin{aligned} y(t) &= [A \odot B]s(t) + n(t), \\ &= Cs(t) + n(t), \end{aligned} \quad (6)$$

where the symbol  $\odot$  stands for the Khatri-Rao product,  $s(t) = [s_1(t), s_2(t), \dots, s_K(t)]^T$ , and  $C = A \odot B$ . Suppose that the noise  $n(t)$  is uncorrelated with the signal  $s(t)$ ; then, the covariance matrix of  $y(t)$  is given by

$$\begin{aligned} R &= E\{y(t)y^H(t)\}, \\ &= CR_s C^H + R_n, \\ &= \tilde{R} + R_n, \end{aligned} \quad (7)$$

where  $E\{\cdot\}$  is to acquire the mathematical expectation and  $(\cdot)^H$  denotes Hermitian transpose.  $R_s = E\{s(t)s^H(t)\}$ ,  $R_n = E\{n(t)n^H(t)\}$ , and  $\tilde{R} = CR_s C^H$ . In the presence of uncorrelated source signals,  $R_s = \text{diag}\{\lambda_1, \lambda_2, \dots, \lambda_K\}$ , where  $\text{diag}\{\cdot\}$  accounts for the diagonalization operation and  $\lambda_k$  is the power of the  $k$ -th source. Moreover, since the noise is nonuniform, its covariance matrix is then given by

$$R_n = \text{diag}\{\sigma_1^2, \sigma_2^2, \dots, \sigma_{6N}^2\}, \quad (8)$$

where  $\sigma_{6(n-1)+q}^2$  denotes the noise power corresponding to the  $q$ -th component of the  $n$ -th EMVS. In practical applications, we can estimate  $R$  via  $L$  samples as

$$\hat{R} = \frac{1}{L} \sum_{t=1}^L y(t)y^H(t). \quad (9)$$

Our objective here is to estimate the angles from  $\hat{R}$ .

### 3. The Proposed Approach

**3.1. Principle of Traditional Eigendecomposition.** It is well known that when Gaussian white noise (uniform noise) exists, the noise powers fulfill

$$\sigma_1^2 = \sigma_2^2 = \dots = \sigma_{6N}^2 = \sigma^2, \quad (10)$$

where  $\sigma^2$  is a constant, and then, the noise covariance becomes

$$R_n = \sigma^2 I_{6N}, \quad (11)$$

where  $I_M$  stands for the  $M \times M$  identity matrix. If we ignore the noise item in equation (7), the eigendecomposition of  $R$  is given by

$$\begin{aligned} \tilde{R} &= \sum_{k=1}^K \alpha_k u_k u_k^H, \\ &= U_s \Sigma_s U_s^H, \end{aligned} \quad (12)$$

where  $\alpha_k$  is the  $k$ -th eigenvalue,  $u_k$  is the associated eigenvector, and  $u_{k_1}^H u_{k_2} = 0$  is for any  $k_1 \neq k_2$ ;  $\Sigma_s = \text{diag}\{\alpha_1, \alpha_2, \dots, \alpha_K\}$  denotes the eigenvalue matrix, and  $U_s = [u_1, u_2, \dots, u_K] \in \mathbb{C}^{6N \times K}$  is called the signal subspace, which spans the same subspace as  $A \odot B$ . Namely, there is a full-rank matrix  $T \in \mathbb{C}^{K \times K}$  such that

$$U_s = CT. \quad (13)$$

Also, the noiseless covariance matrix can be expressed as

$$\begin{aligned} \tilde{R} &= \sum_{k=1}^K \alpha_k u_k u_k^H + \sum_{n=1}^{6N-K} 0 \cdot v_n v_n^H, \\ &= U_s \Sigma_s U_s^H + U_n 0_{(6N-K) \times (6N-K)} U_n^H, \end{aligned} \quad (14)$$

where  $v_n$  is the eigenvector from the null subspace of  $U_s$ , i.e.,  $v_n^H U_s = 0_{1 \times K}$ , and  $0_{M \times N}$  represents the  $M \times N$  full zero matrix.  $\Sigma_s = \text{diag}\{\alpha_1 + \sigma^2, \alpha_2 + \sigma^2, \dots, \alpha_K + \sigma^2\}$ , and  $U_n = [v_1, v_2, \dots, v_{6N-K}] \in \mathbb{C}^{6N \times (6N-K)}$  is called the noise subspace. Since the identity matrix can be formulated as the product of arbitrary unitary matrix and its Hermitian transpose, the noisy  $R$  can be written as

$$\begin{aligned} R &= \sum_{k=1}^K (\alpha_k + \sigma^2) u_k u_k^H + \sum_{n=1}^{6N-K} \sigma^2 u_n u_n^H, \\ &= U_s \Sigma_s U_s^H + U_n \Sigma_n U_n^H, \end{aligned} \quad (15)$$

where  $\Sigma_n = \text{diag}\{\sigma^2, \sigma^2, \dots, \sigma^2\} \in \mathbb{C}^{(6N-K) \times (6N-K)}$ . The results in equation (15) reveal that the uniform noise would not destroy the eigendistribution of the signal. However, in the presence of nonuniform noise, the noise power is not unique, so the conclusion in equation (15) will be untenable. It is necessary for us to denoise before further processing.

**3.2. Denoising.** Let  $\Omega$  be a set that records the nonzero entities of  $R_n$ , i.e.,

$$\Omega = \{(m, m) | m = 1, 2, \dots, 6N\}. \quad (16)$$

We define a sampling operator  $S_\Omega\{\cdot\}$  that picks up the elements of the matrix in the blanket with indexes in  $\Omega$ , for example,  $S_\Omega\{R\} = \bar{R} \in \mathbb{C}^{6N \times 6N}$  such that

$$\bar{R}(m, n) = \begin{cases} R(m, n), & (m, n) \in \Omega, \\ 0, & (m, n) \notin \Omega, \end{cases} \quad (17)$$

where  $R(m, n)$  denotes the  $(m, n)$ -th entity of  $R$  and is similar to others. Since  $R_n$  is a diagonal matrix, we have  $R_n = S_\Omega\{R_n\}$ . The effect of the noise can be easily removed via the following reduced covariance matrix:

$$\begin{aligned} \tilde{R} &= R - S_\Omega\{R\}, \\ &= \tilde{R} - S_\Omega\{\tilde{R}\}. \end{aligned} \quad (18)$$

The abovementioned denoising procedure is illustrated in Figure 1. However, the abovementioned denoising procedure can also destroy the structure of  $\tilde{R}$ , so we need to recover  $\tilde{R}$  from  $\bar{R}$ . Next, let us focus on the diagonal element of  $\tilde{R}$ . It can be deduced that the  $m$ -th ( $m = 6(n-1) + q$ ) diagonal entity of  $\tilde{R}$  is

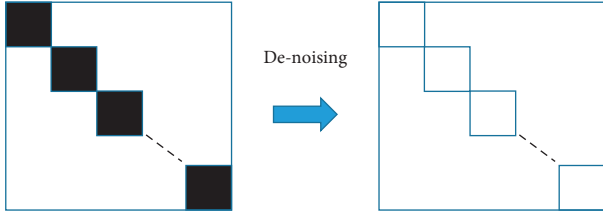


FIGURE 1: Illustration of the proposed denoising principle.

$$\begin{aligned}
 \tilde{R}(m, m) &= \sum_{k=1}^K C(m, k) \lambda_k C^H(m, k), \\
 &= \sum_{k=1}^K |C(m, k)|^2 \lambda_k, \\
 &= \sum_{k=1}^K \left| e^{-j\pi\tau_{n,k}} B(q, k) \right|^2 \lambda_k, \\
 &= \sum_{k=1}^K |B(q, k)|^2 \lambda_k.
 \end{aligned} \tag{19}$$

We define  $\chi_q = \sum_{k=1}^K |B(q, k)|^2 \lambda_k$  and let  $\chi = \text{diag}\{\chi_1, \chi_2, \dots, \chi_6\} \in \mathbb{C}^{6 \times 6}$ , and then, we have

$$\tilde{R} = R_s - I_6 \otimes \chi. \tag{20}$$

Since  $R_s$  is a low-rank matrix, the noiseless recovery problem can be formulated as [32]

$$\begin{aligned}
 \min \text{rank}\{R\} \\
 \text{s.t. } S_\Omega(R) = \tilde{R},
 \end{aligned} \tag{21}$$

where  $\text{rank}\{R\}$  returns the rank of  $R$ . To recover, the noiseless covariance coincides with the concept of matrix completion. Noting that the rank optimization is a non-convex issue, it is usually replaced by the relaxed nuclear norm constraint  $\|\cdot\|_*$ , i.e.,

$$\begin{aligned}
 \min \|R\|_* \\
 \text{s.t. } S_\Omega(R) = \tilde{R}.
 \end{aligned} \tag{22}$$

In practice,  $\tilde{R}$  is replaced by its estimation, denoted by  $\hat{R}_1$ . Since there exists error between  $R$  and  $\hat{R}_1$ , a bound is usually set, and the issue in equation (22) is transformed into

$$\begin{aligned}
 \min \|R\|_* \\
 \text{s.t. } \|S_\Omega(R) - \hat{R}_1\| \leq \varepsilon.
 \end{aligned} \tag{23}$$

In practice,  $\varepsilon$  is usually chosen according to the noise tolerance; in this paper, it is set to  $10^{-4}$ . The abovementioned optimization can be easily accomplished via the convex toolboxes, e.g., cvx. After that, the eigendecomposition can be performed, and then, the estimation of the signal subspace  $U_s$  is accomplished.

3.3. Parameter Estimation. Actually, the following rotational invariance relations exist:

$$\begin{cases}
 AD_1\{B\} = AD_2\{B\}\Phi^{(1,2)}, \\
 AD_1\{B\} = AD_3\{B\}\Phi^{(1,3)}, \\
 \vdots \\
 AD_1\{B\} = AD_6\{B\}\Phi^{(1,6)},
 \end{cases} \tag{24}$$

where  $D_n\{B\}$  returns a diagonal matrix, the diagonals of which are the  $n$ -th row of  $B$ , and  $\Phi^{(1,q)} = \text{diag}\{\beta_1^{(1,q)}, \beta_2^{(1,q)}, \dots, \beta_K^{(1,q)}\}$ ,  $q = 2, 3, \dots, 6$ ,  $\beta_k^{(1,q)} = b_k(q)/b_k(1)$ . Next, we define

$$J_q = I_M \otimes i_{6,q}, \tag{25}$$

where  $i_{6,q}$  accounts for the  $q$ -th column of  $I_6$ . The relations in equation (24) become

$$\begin{cases}
 J_1[A \odot B] = J_2[A \odot B]\Phi^{(1,2)}, \\
 J_1[A \odot B] = J_3[A \odot B]\Phi^{(1,3)}, \\
 \vdots \\
 J_1[A \odot B] = J_6[A \odot B]\Phi^{(1,6)}.
 \end{cases} \tag{26}$$

Inserting equation (26) into equation (13) yields

$$\begin{cases}
 J_1 U_s = J_2 U_s T^{-1} \Phi^{(1,2)} T, \\
 J_1 U_s = J_3 U_s T^{-1} \Phi^{(1,3)} T, \\
 \vdots \\
 J_1 U_s = J_6 U_s T^{-1} \Phi^{(1,6)} T,
 \end{cases} \tag{27}$$

where  $(\cdot)^{-1}$  denotes the inverse. In other words, we have

$$\begin{cases}
 (J_2 U_s)^\dagger J_1 U_s = T^{-1} \Phi^{(1,2)} T, \\
 T (J_3 U_s)^\dagger J_1 U_s T^{-1} = \Phi^{(1,3)}, \\
 \vdots \\
 T (J_6 U_s)^\dagger J_1 U_s T^{-1} = \Phi^{(1,6)},
 \end{cases} \tag{28}$$

where the superscript  $(\cdot)^\dagger$  denotes the pseudoinverse. Performing eigendecomposition on  $(J_2 U_s)^\dagger J_1 U_s$ , we can get the eigenvalues of the matrix and the associated eigenvectors, which reveal the estimation of  $\Phi^{(1,2)}$  and the estimation of  $T$  (denoted as  $\hat{T}$ ). Calculating the left parts of equation (28) (except the first row), one can get the estimation of  $\Phi^{(1,3)}$ ,  $\Phi^{(1,4)}$ ,  $\Phi^{(1,5)}$ , and  $\Phi^{(1,6)}$ , respectively.

It has been pointed out in [20] that  $b_k$  can be written as

$$b_k = b_k(1) \begin{bmatrix} 1 \\ \beta_k^{(1,2)} \\ \vdots \\ \beta_k^{(1,6)} \end{bmatrix}. \tag{29}$$

It is easy to find that



$$\left( b_k(1) \begin{bmatrix} 1 \\ \beta_k^{(1,2)} \\ \beta_k^{(1,3)} \end{bmatrix} \right) * \left( b_k(1) \begin{bmatrix} \beta_k^{(1,4)} \\ \beta_k^{(1,5)} \\ \beta_k^{(1,6)} \end{bmatrix} \right)^* = \|b_k(1)\|^2 \left( \begin{bmatrix} 1 \\ \beta_k^{(1,2)} \\ \beta_k^{(1,3)} \end{bmatrix} * \begin{bmatrix} \beta_k^{(1,4)} \\ \beta_k^{(1,5)} \\ \beta_k^{(1,6)} \end{bmatrix} \right)^* \quad (30)$$

Let  $e_k = [b_k(1), b_k(2), b_k(3)]^T$  and  $h_k = [b_k(4), b_k(5), b_k(6)]^T$ . Then, we have

$$\frac{e_k}{\|e_k\|} * \frac{h_k^*}{\|h_k\|} = \begin{bmatrix} \sin \theta_k \cos \phi_k \\ \sin \theta_k \sin \phi_k \\ \cos \theta_k \end{bmatrix}. \quad (31)$$

According to equation (30), we can get

$$\begin{bmatrix} u_k \\ v_k \\ w_k \end{bmatrix} \triangleq \left( \frac{b_k(1)b_k^*(1)}{\|b_k(1)\|\|b_k^*(1)\|} \right) \cdot \frac{\begin{bmatrix} 1 \\ \beta_k^{(1,2)} \\ \beta_k^{(1,3)} \end{bmatrix}}{\| \begin{bmatrix} 1 \\ \beta_k^{(1,2)} \\ \beta_k^{(1,3)} \end{bmatrix} \|} * \frac{\begin{bmatrix} \beta_k^{(1,4)} \\ \beta_k^{(1,5)} \\ \beta_k^{(1,6)} \end{bmatrix}}{\| \begin{bmatrix} \beta_k^{(1,4)} \\ \beta_k^{(1,5)} \\ \beta_k^{(1,6)} \end{bmatrix} \|},$$

$$\triangleq \frac{\begin{bmatrix} 1 \\ \beta_k^{(1,2)} \\ \beta_k^{(1,3)} \end{bmatrix}}{\| \begin{bmatrix} 1 \\ \beta_k^{(1,2)} \\ \beta_k^{(1,3)} \end{bmatrix} \|} * \frac{\begin{bmatrix} \beta_k^{(1,4)} \\ \beta_k^{(1,5)} \\ \beta_k^{(1,6)} \end{bmatrix}}{\| \begin{bmatrix} \beta_k^{(1,4)} \\ \beta_k^{(1,5)} \\ \beta_k^{(1,6)} \end{bmatrix} \|},$$

$$= \begin{bmatrix} \sin \theta_k \cos \phi_k \\ \sin \theta_k \sin \phi_k \\ \cos \theta_k \end{bmatrix}. \quad (32)$$

Obviously,  $\|b_k(1)\|^2$  is a constant, and it has been removed by normalizing calculation. Let the estimations of  $u_k$ ,  $v_k$ , and  $w_k$  be  $\hat{u}_k$ ,  $\hat{v}_k$ , and  $\hat{w}_k$ , respectively. 2D-DOA can be estimated by

$$\begin{cases} \hat{\theta}_k = \arccos(\hat{w}_k), \\ \hat{\phi}_k = \arctan(\hat{v}_k/\hat{u}_k). \end{cases} \quad (33)$$

Once the 2D-DOA estimation has been accomplished, the polarization parameters can be estimated via the least squares approach in [30]. The details are omitted for simplicity.

## 4. Algorithmic Analyses

### 4.1. Important Remarks

Remark 1: as described in the context, the proposed method is insensitive to the  $r_n$ , which means it is suitable for arbitrary sensor geometry. Besides, it is insensitive to the sensor position error as well.

Remark 2: it is well known that the uniform noise is a special case of the nonuniform noise. Therefore, the proposed algorithm is effective in the white noise scenario.

Remark 3: as explained in [30], all the estimated parameters  $\theta_k, \phi_k, \eta_k, \gamma_k$  are one-to-one paired.

Remark 4: since the matrix completion would not hurt the rank and the dimension of the covariance matrix, the proposed algorithm can identify the same number of sources in [20].

4.2. Stochastic CRB. Let  $R_n = Q(q)$ , where  $q = [q_1, q_2 \dots q_P]^T$  is a real vector that parameterizes  $R_n$ . From the derivations in [35], we can get the stochastic CRB on 2D-DOA and polarization angle, which are given by

$$\text{CRB} = \frac{1}{L} [H - MT^{-1}M^T]^{-1}, \quad (34)$$

with

$$\begin{cases} H = 2\text{Re} \left\{ \left( \tilde{D}^H \prod_F^{-\perp} \tilde{D} \right) \otimes \left( R_c \tilde{F}^H \tilde{R}^{-1} \tilde{F} R_c \right) \right\} \otimes 1_{4 \times 4}, \\ M = 2\text{Re} \left\{ \begin{bmatrix} J^T \left( \left( \tilde{D}^H \prod_F^{-\perp} \right) \otimes \left( \tilde{R}^{-1} \tilde{F} R_c \right)^T \right) \tilde{Q}^* \\ J^T \left( \left( \tilde{D}^H \prod_F^{-\perp} \right) \otimes \left( \tilde{R}^{-1} \tilde{F} R_c \right)^T \right) \tilde{Q}^* \end{bmatrix} \right\}, \\ T = 2\text{Re} \left\{ \tilde{Q}^H \left( \tilde{R}^{-T} \otimes \prod_F^{-\perp} \right) \tilde{Q} \right\} - \tilde{Q}^H \left( \left( \prod_F^{-\perp} \right)^T \otimes \prod_F^{-\perp} \right) \tilde{Q}. \end{cases} \quad (35)$$

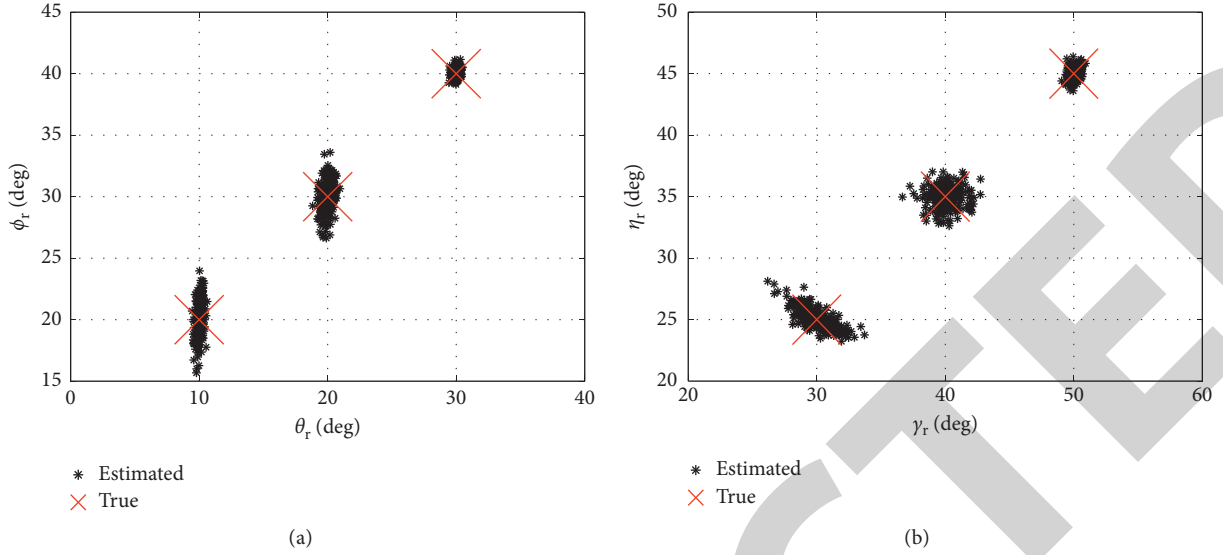


FIGURE 2: Scattering figures of our algorithm with  $N=4$ ,  $L=500$ , and  $\text{SNR}=20$  dB: (a) 2D-DOA estimation; (b) polarization parameter estimation.

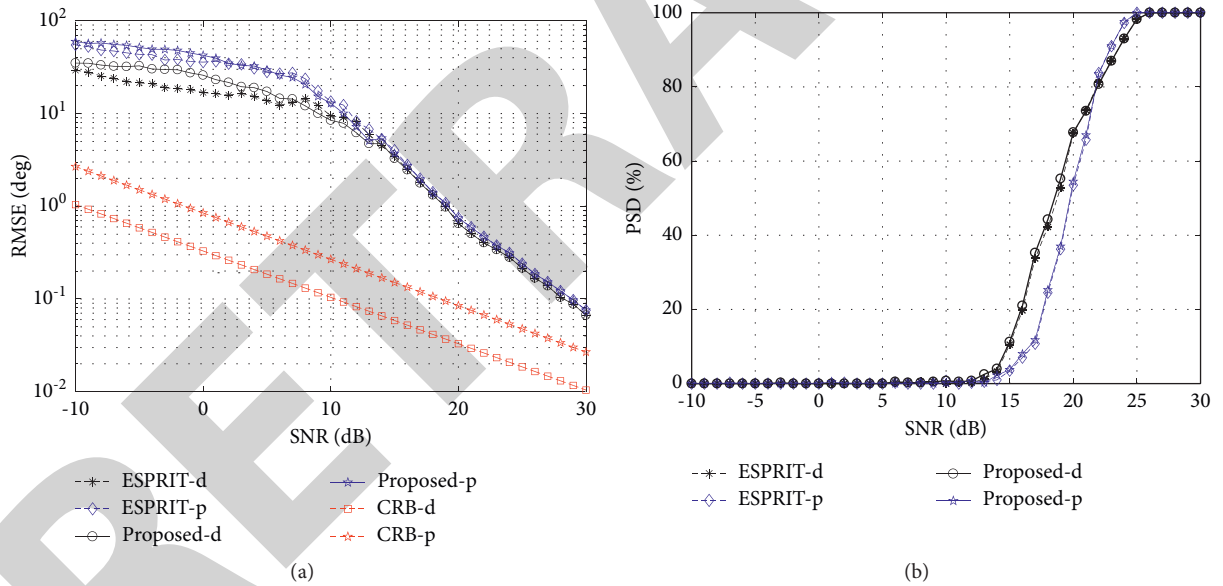


FIGURE 3: RMSE performance and PSD performance versus SNR (a) RMSE vs. SNR (b) PSD vs. SNR.

where  $\tilde{F} = Q^{-1/2}C$ ,  $\Pi_F^\perp = I_{6N} - \Pi_F$  with  $\Pi_F = \tilde{F}\tilde{F}^\dagger$ , And  $\tilde{D} = [\tilde{D}_d, \tilde{D}_p]$ , where  $\tilde{D}_d = Q^{-1/2}D_d$  and  $\tilde{D}_p = Q^{-1/2}D_p$  with  $D_d = [\partial f_1/\partial\theta_1, \dots, \partial f_K/\partial\theta_K, \partial f_1/\partial\phi_1, \dots, \partial f_K/\partial\phi_K]$  and  $D_p = [\partial f_1/\partial\eta_1, \dots, \partial f_K/\partial\eta_K, \partial f_1/\partial\gamma_1, \dots, \partial f_K/\partial\gamma_K]$ , respectively, where  $f_k$  denotes that with the  $k$ -th column of  $C$ .  $\tilde{R} = Q^{-1/2}RQ^{-1/2}$ .  $J = [\text{vec}\{e_1e_1^T\}, \text{vec}\{e_2e_2^T\}, \dots, \text{vec}\{e_Ke_K^T\}]$ , where  $e_k$  denotes the  $k$ -th column of  $I_K$  and  $\text{vec}\{\cdot\}$  denotes the vectorization.  $\tilde{Q} = [\text{vec}\{\tilde{Q}'_1\}, \text{vec}\{\tilde{Q}'_2\}, \dots, \text{vec}\{\tilde{Q}'_p\}]$  with  $\tilde{Q}'_p = Q^{-1/2}Q'_pQ^{-1/2}$ ,  $\tilde{Q}'_p = \partial Q/\partial q_p$ .

## 5. Simulation Results

In this subsection, the Monte Carlo simulation is utilized to assess the estimation accuracy. We consider an arbitrary  $N$ -element EMVS receives array configuration, and we assume that  $K=3$  far-field sources impinge on the array, whose parameters are  $\theta = (10^\circ, 20^\circ, 30^\circ)$ ,  $\phi = (20^\circ, 30^\circ, 40^\circ)$ ,  $\gamma = (0^\circ, 40^\circ, 50^\circ)$ , and  $\eta = (25^\circ, 35^\circ, 45^\circ)$ . Moreover, we suppose that  $L$  snapshots have been collected. Each result

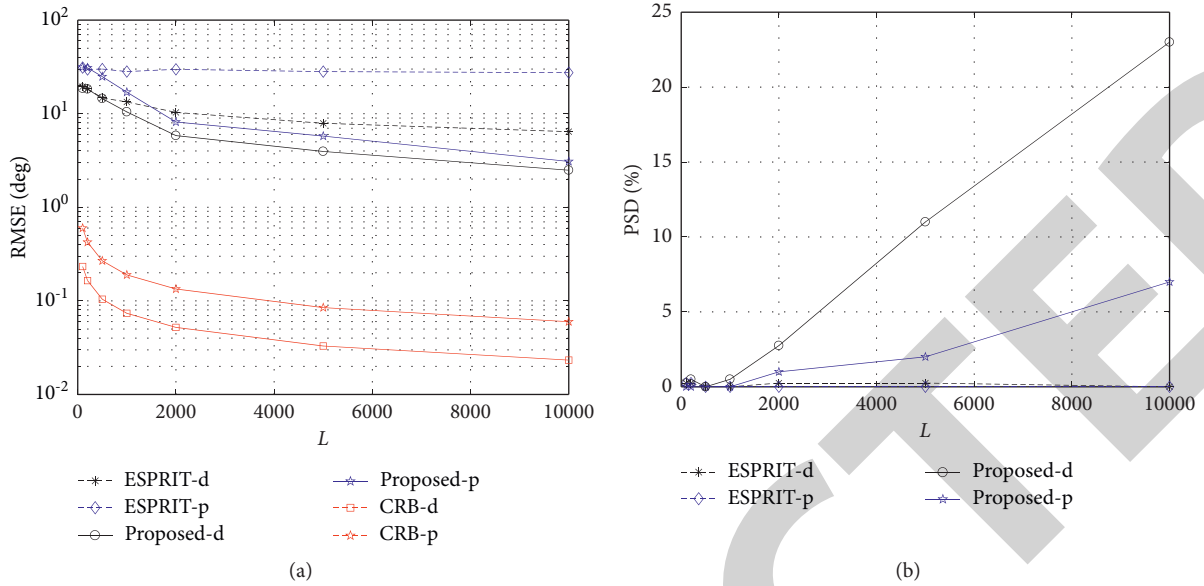


FIGURE 4: RMSE performance and PSD performance versus  $L$  (a) RMSE vs.  $L$  (b) PSD vs.  $L$ .

relies on 200 experiments. In the simulation, the signal-to-noise ratio (SNR) is defined as the ration of the power of the two components in equation (6). Two measures are adopted: one is the root mean square error (RMSE), and the other is the probability of successful detection (PSD). In all the simulations, the noise is randomly generated with powers which are uniformly chosen from  $[1 \ 100000]$ .

*Example 1.* We give the scattering figures of the proposed algorithm with  $N=4$  and  $L=500$ , where the SNR is set to 20 dB. Herein, the EMVS is randomly placed in a three-dimensional space with  $(x_n, y_n, z_n)$  fulfilling a uniform distribution with interval  $[-0.5\lambda, 0.5\lambda]$ . Figure 2 shows the results of direction angle estimation and polarization parameters estimation. Clearly, all the angles can be correctly estimated and automatically paired. It is evident that our estimator is effective in a nonuniform noise scenario.

*Example 2.* We present the RMSE and PSD curves of the proposed estimator. Herein, a successful trial is recognized if the absolute error of the estimated angle is smaller than  $1^\circ$ . In Figure 3, we plot the average estimation performance on the direction angle estimate (labelled with the suffix “-d”) and polarization angle estimate (labelled with the suffix “-p”), where  $N=4$  and  $L=500$ . In contrast, the RMSE results of ESPRIT in [20] as well as the CRB are added. From the result, we can observe that the RMSE performance of both the proposed estimator and ESPRIT is improved with the increasing SNR, while the PSD of both estimators reaches 100%, once SNR is larger than a threshold (e.g., 25 dB). Besides, it depicts that the proposed estimator provides more accurate parameter estimation performance for direction angle estimation when  $\text{SNR} < 10$  dB. However, the improvement is not obvious as for polarization parameter estimation.

*Example 3.* We plot the average RMSE performance and the average PSD curves with different snapshot number  $L$  in Figure 4, while  $N$  and SNR are set to 4 and 10 dB, respectively. Notably, both the proposed estimator and ESPRIT provide better estimation performance with larger  $L$ . Similar to the previous observation, the proposed algorithm outperforms the ESPRIT algorithm. The improvement benefits from the fact that the proposed algorithm can eliminate the noise, while traditional ESPRIT algorithm cannot avoid the effect of nonuniform noise.

## 6. Conclusions

In this paper, we investigate the issue of angle estimation using EMVS array with arbitrary sensor geometry and nonuniform noise. A matrix completion-based algorithm has been proposed, which first eliminates the effect of nonuniform via solving a convex problem. After the noiseless covariance matrix has been recovered, the traditional subspace method is utilized to estimate the signal subspace, and the ESPRIT idea is adopted for 2D-DOA estimation. Our algorithm is robust to nonuniform noise and sensor position error. It should be pointed out that the tensor structure has not been exploited. More attention should be paid to this topic to further increase the estimation accuracy.

## Data Availability

No data were used in this study.

## Conflicts of Interest

The authors declare no conflicts of interest.



## Acknowledgments

This work was supported by the National Natural Science Foundation of China under Grant no. 62071476.

## References

- [1] G. Gui, M. Liu, F. Tang, N. Kato, and F. Adachi, "6G: opening new horizons for integration of comfort, security, and intelligence," *IEEE Wireless Communications*, vol. 27, no. 5, pp. 126–132, 2020.
- [2] H. Wang, L. Xu, Z. Yan, and T. A. Gulliver, "Low-complexity MIMO-FBMC sparse channel parameter estimation for industrial big data communications," *IEEE Transactions on Industrial Informatics*, vol. 17, no. 5, pp. 3422–3430, 2021.
- [3] H. Wang, X. Li, R. H. Jhaveri et al., "Sparse bayesian learning based channel estimation in FBMC/OQAM industrial IoT networks," *Computer and Communications*, vol. 17, pp. 40–45, 2021.
- [4] L. Wan, K. Liu, Y.-C. Liang, and T. Zhu, "DOA and polarization estimation for non-circular signals in 3-D millimeter wave polarized massive MIMO systems," *IEEE Transactions on Wireless Communications*, vol. 20, no. 5, pp. 3152–3167, 2021.
- [5] D. Chen, B. Chen, and G. Qin, "Angle estimation using ESPRIT in MIMO radar," *Electronics Letters*, vol. 44, no. 12, pp. 770–771, 2008.
- [6] J. Chen, H. Gu, and W. Su, "Angle estimation using ESPRIT without pairing in MIMO radar," *Electronics Letters*, vol. 44, no. 24, pp. 1422–1423, 2008.
- [7] I. Bekkerman and J. Tabrikian, "Target detection and localization using MIMO radars and sonars," *IEEE Transactions on Signal Processing*, vol. 54, no. 10, pp. 3873–3883, 2006.
- [8] H. Yan, J. Li, and G. Liao, "Multitarget identification and localization using bistatic MIMO radar systems," *EURASIP Journal on Applied Signal Processing*, vol. 2008, Article ID 8828610, 2008.
- [9] X. Zhang, L. Xu, L. Xu, and D. Xu, "Direction of departure (DOD) and direction of arrival (DOA) estimation in mimo radar with reduced-dimension music," *IEEE Communications Letters*, vol. 14, no. 12, pp. 1161–1163, 2010.
- [10] Z. D. Zheng and J. Y. Zhang, "Fast method for multi-target localisation in bistatic MIMO radar," *Electronics Letters*, vol. 47, no. 2, pp. 138–139, 2011.
- [11] B. Tang, J. Tang, Y. Zhang, and Z. Zheng, "Maximum likelihood estimation of DOD and DOA for bistatic MIMO radar," *Signal Processing*, vol. 93, no. 5, pp. 1349–1357, 2013.
- [12] Y. Cheng, R. Yu, H. Gu, and W. Su, "Multi-SVD based subspace estimation to improve angle estimation accuracy in bistatic MIMO radar," *Signal Processing*, vol. 93, no. 7, pp. 2003–2009, 2013.
- [13] X. Zhang, Z. Xu, L. Xu, and D. Xu, "Trilinear decomposition-based transmit angle and receive angle estimation for multiple-input multiple-output radar," *IET Radar, Sonar & Navigation*, vol. 5, no. 6, pp. 626–631, 2011.
- [14] J. Shi, F. Wen, and T. Liu, "Nested MIMO radar: coarrays, tensor modeling and angle estimation," *IEEE Transactions on Aerospace and Electronic Systems*, vol. 57, no. 1, pp. 573–585, 2021.
- [15] W. Rao, D. Li, and J. Q. Zhang, "A tensor-based approach to L-shaped arrays processing with enhanced degrees of freedom," *IEEE Signal Processing Letters*, vol. 25, no. 2, pp. 234–238, 2018.
- [16] R. Goossens and H. Rogier, "A hybrid UCA-RARE/Root-MUSIC approach for 2-D direction of arrival estimation in uniform circular arrays in the presence of mutual coupling," *IEEE Transactions on Antennas and Propagation*, vol. 55, no. 3, pp. 841–849, 2007.
- [17] M. D. Zoltowski, M. Haardt, and C. P. Mathews, "Closed-form 2-D angle estimation with rectangular arrays in element space or beamspace via unitary ESPRIT," *IEEE Transactions on Signal Processing*, vol. 44, no. 2, pp. 316–328, 1996.
- [18] J. He, L. Li, and T. Shu, "Sparse nested arrays with spatially spread orthogonal dipoles: high accuracy passive direction finding with less mutual coupling," *IEEE Transactions on Aerospace and Electronic Systems*, 2021.
- [19] K. T. Wong and X. Yuan, "Vector cross-product direction-finding with an electromagnetic vector-sensor of six orthogonally oriented but spatially noncollocating dipoles/loops," *IEEE Transactions on Signal Processing*, vol. 59, no. 1, pp. 160–171, 2011.
- [20] K. T. Wong and M. D. Zoltowski, "Closed-form direction finding and polarization estimation with arbitrarily spaced electromagnetic vector-sensors at unknown locations," *IEEE Transactions on Antennas and Propagation*, vol. 48, no. 5, pp. 671–681, 2000.
- [21] A. Nehorai and E. Paldi, "Vector-sensor array processing for electromagnetic source localization," *IEEE Transactions on Signal Processing*, vol. 42, no. 2, pp. 376–398, 1994.
- [22] J. Li, "Direction and polarization estimation using arrays with small loops and short dipoles," *IEEE Transactions on Antennas and Propagation*, vol. 41, no. 3, pp. 379–387, 1993.
- [23] K. T. Wong and M. D. Zoltowski, "Uni-vector-sensor ESPRIT for multisource azimuth, elevation, and polarization estimation," *IEEE Transactions on Antennas and Propagation*, vol. 45, no. 10, pp. 1467–1474, 1997.
- [24] K. T. Wong and M. D. Zoltowski, "Self-initiating music-based direction finding and polarization estimation in spatio-polarizational beamspace," *IEEE Transactions on Antennas and Propagation*, vol. 48, no. 8, pp. 1235–1245, 2000.
- [25] M. D. Zoltowski and K. T. Wong, "ESPRIT-based 2-D direction finding with a sparse uniform array of electromagnetic vector sensors," *IEEE Transactions on Signal Processing*, vol. 48, no. 8, pp. 2195–2204, 2000.
- [26] S. Miron, N. Le Bihan, and J. Mars, "Vector-sensor MUSIC for polarized seismic sources localization," *EURASIP Journal on Applied Signal Processing*, vol. 48, no. 8, Article ID 280527, 2005.
- [27] J. He and Z. Liu, "Computationally efficient 2D direction finding and polarization estimation with arbitrarily spaced electromagnetic vector sensors at unknown locations using the propagator method," *Digital Signal Processing*, vol. 19, no. 3, pp. 491–503, 2009.
- [28] T. Ahmed, Z. Xiaofei, and Z. Wang, "DOA estimation for coprime EMVS arrays via minimum distance criterion based on PARAFAC analysis," *IET Radar, Sonar & Navigation*, vol. 13, no. 1, pp. 65–73, 2019.
- [29] S. Chintagunta and P. Palanisamy, "2D-DOD and 2D-DOA estimation using the electromagnetic vector sensors," *Signal Processing*, vol. 147, pp. 163–172, 2018.
- [30] F. Wen, J. Shi, and Z. Zhang, "Closed-form estimation algorithm for EMVS-MIMO radar with arbitrary sensor geometry," *Signal Processing*, vol. 186, Article ID 108117, 2021.
- [31] X. Wang, M. Huang, and L. Wan, "Joint 2D-DOD and 2D-DOA estimation for coprime EMVS-MIMO radar," *Circuits, Systems, and Signal Processing*, 2021.

- [32] B. Liao, H. Lei, C. Guo et al., "New approaches to direction-of-arrival estimation with sensor arrays in unknown non-uniform noise," *IEEE Sensors Journal*, vol. 16, no. 24, pp. 8982–8989, 2016.
- [33] B. Liao, S. C. Chan, H. Lei et al., "Iterative methods for subspace and DOA estimation in nonuniform noise," *IEEE Transactions on Signal Processing*, vol. 64, no. 12, pp. 3008–3020, 2016.
- [34] B. Liao, "Fast angle estimation for MIMO radar with non-orthogonal waveforms," *IEEE Transactions on Aerospace and Electronic Systems*, vol. 54, no. 4, pp. 2091–2096, 2018.
- [35] M. Pesavento and A. B. Gershman, "Maximum-likelihood direction-of-arrival estimation in the presence of unknown nonuniform noise fields," *IEEE Transactions on Signal Processing*, vol. 49, no. 7, pp. 1310–1324, 2001.

RETRACTED